Diffuse X-Ray Scattering Study of an Oxygen-Disordered Tetragonal $YBa_2(Cu_{0.955}Al_{0.045})_3O_7$ Crystal

X. Jiang,[1] P. Wochner,[1] S. C. Moss,[1] and P. Zschack[2]

[1]*Physics Department and Texas Center for Superconductivity, University of Houston, Houston, Texas 77204-5504*

[2]*Oak Ridge Associated Universities at the National Synchrotron Light Source, Line X14, Brookhaven National Laboratory, Upton, New York 11973*

(Received 22 April 1991)

X-ray scattering from a tetragonal single crystal of $YBa_2(Cu_{0.955}Al_{0.045})_3O_7$ shows diffuse streaking in [110] directions about the Bragg peaks. Through a quantitative calculation using a coupled concentration wave, static displacement wave approach, we show that this is essentially attributable to the shear displacement field produced by a disordered oxygen array on the Cu(1)-O "chain" plane. We also observe pronounced short-range chain order (local orthorhombic fluctuations) whose correlation range is considerably greater than the superconducting coherence length. This suggests that on a scale relevant for superconductivity the (local) orthorhombicity remains important in this tetragonal structure.

PACS numbers: 61.10.−i, 61.70.Bv, 74.60.Mj

In the high-T_c superconductor $YBa_2Cu_3O_{7-\delta}$, there are two distinct Cu-oxide layers—the Cu(1)-O chain plane and the Cu(2)-O_2 plane. While the latter seems to play an essential role, much discussion has also been devoted to the role of the oxygen chains in the Cu(1)-O planes and to the role of orthorhombicity. In particular, compounds of the form $YBa_2(Cu_{1-x}M_x)_3O_7$ (M=Al, Co, Ga, or Fe) have been intensively studied and show, with increasing x, a decrease in the orthorhombic distortion [1–8], leading to an orthorhombic-to-tetragonal phase transition at $x_c \simeq 0.04$ (M=Al). Above x_c, however, high-T_c values persist in these compounds, disappearing only for substantial x (>0.10). It has been determined by a variety of experiments [6–13] that Al, Co, and Fe substitute initially in the Cu(1) positions, thereby disordering the chains to produce the phase transition. Below x_c there are characteristic twin-spot splittings in the electron-diffraction patterns which merge into diffuse reflections as x_c is approached. At $x > x_c$ electron diffraction has shown crossed diffuse scattering patterns around the tetragonal Bragg peaks [14–17] with streaks in the $\langle 110\rangle$ or $\langle 1\bar{1}0\rangle$ directions (the split-spot directions below x_c), and a domainlike "tweed" contrast in the transmission-electron-microscope (TEM) images.

Currently, two microtwin models [8,17–21] have been invoked to explain the above results for $x > x_c$ in which the trivalent impurities may either act as the twin centers [17,19,20] or cluster along the twin boundaries [8,21]. Both models consider each twin domain to possess an orthorhombic structure with Cu-O chains along either the $\langle 010\rangle$ or the $\langle 100\rangle$ direction and with twin boundaries along $\langle 1\bar{1}0\rangle$ and $\langle 110\rangle$. Below x_c, such a domain description would seem to be appropriate. Above x_c, the mixed-orientation array of microdomains must, however, lead to a single coherent average tetragonal structure with sharp (unsplit) Bragg spots.

The detailed atomic arrangements resulting from these substitutional defects is still unknown because there has been no quantitative analysis of the diffuse scattering patterns. In this Letter we present such data along with a theoretical analysis using concentration and static displacement wave methods [22]. A principal conclusion is that the dominant contribution to the observed scattering, aside from the thermal vibrations (which show no unusual shear softness [23]), comes from the static displacements arising from a disordered array of elastic (Cu-O-Cu) dipoles. While microdomains are not required as a descriptive aid and the TEM "tweed" structures can be, as in other examples of *premonitory* structural fluctuations [24], attributed to these displacement fields, we nonetheless observe appreciable orthorhombic fluctuations above x_c which are correlated over distances considerably greater than the superconducting coherence length [25].

Single crystals of $YBa_2(Cu_{1-x}Al_x)_3O_7$ were prepared by Zhu *et al.* [14]. By electron microprobe analysis we determined the x value to range from 0.04 to 0.06 and we chose a crystal with x=0.045 which is just beyond x_c. The crystal plate was then trimmed to $0.6\times0.18\times0.056$ mm^3 so that it could be bathed in the uniform area of an x-ray beam. Using a conventional rotating-anode supply and four-circle diffractometer the tetragonal structure was confirmed, with $a=b=3.8668(11)$ Å and $c=11.7060(35)$ Å, and a full x-ray crystallographic analysis was conducted [16] from which we determined that there is no significant Al content at the Cu(2) sites in agreement with other investigations [6-13]. The x-ray diffuse scattering experiments were carried out on the X14 beam line at the Brookhaven National Synchrotron Light Source. The incident energy, E=16.8 keV, was chosen to be ~230 eV below the yttrium absorption edge to avoid Y fluorescence. The sample was inside a He-filled Be hemisphere to remove air scattering.

Figure 1 illustrates the Q^2 dependence ($Q=4\pi\sin\theta/\lambda$) of the normalized diffuse intensity measured at an identical small deviation $\mathbf{q}$ from the Bragg points (040), (060), (080), and (0100). Each intensity value is normalized by dividing by $|F_{0k0}|^2$, the square of the structure factor determined earlier [16]. In Figs. 2(a)–2(c) are contour plots of the measured diffuse scattering around the (040),

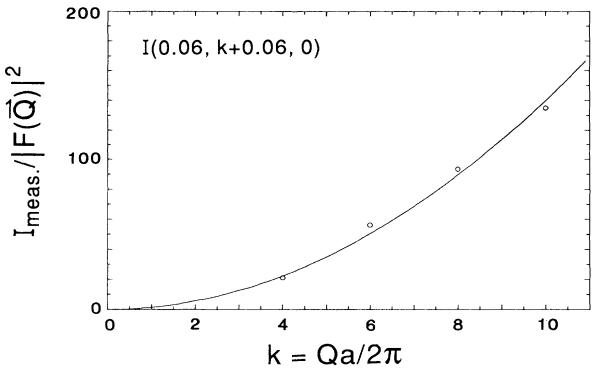

FIG. 1. Measured x-ray intensity divided by $|F(\mathbf{Q})|^2$ at positions $(0.06,k+0.06,0)$ in the vicinity of the $(0k0)$ Bragg peaks (040), (060), (080), and (0100). The solid curve shows the Q^2 dependence required by scattering off atomic displacements.

(240), and (220) reciprocal-lattice points divided by $|F(\mathbf{Q})|^2$. Around $(0k0)$ the diffuse patterns are streaked along the two equivalent [110] directions and the two streaks make equal contributions. Around $(hk0)$, $h\neq k\neq 0$, the $\langle 110\rangle$ diffuse streaks, which make an angle with $\mathbf{Q}$ of less than 45°, diminish and at $(hh0)$ these $\langle 110\rangle$ contributions are radial (parallel to $\mathbf{Q}$) and vanish. These features, characteristic of essentially $\langle 110\rangle$:$\langle 1\bar{1}0\rangle$ shear displacements, differ from the electron diffraction patterns because of multiple scattering [26].

Given the Q^2 dependence of the diffuse intensities in Fig. 1, the experimental results cannot be explained by either pure substitutional disorder or by a microdomain size broadening as in neither case does the normalized diffuse intensity depend on Q. The Q^2 dependence leads us naturally to conclude that our observed scattering results from atomic displacements [22] of a dynamic (thermal) or static origin. The latter could arise from either aluminum substitutions at the Cu(1) sites or a disordered distribution of oxygen in the Cu(1)-O planes. Above x_c, however, increasing the Al concentration has very little effect on the tetragonal lattice parameters [7] and we thus focus our attention on the static displacements attributable to a disordered array of oxygens.

In a disordered lattice (here we have oxygens and vacancies) the displacements $\Delta\mathbf{R}_s$ of *all* of the lattice sites in the long-wave approximation can be written to first order as follows [22]:

$$\Delta\mathbf{R}_s=\sum_{\mathbf{q}}\mathbf{A}_{\mathbf{q}}c_{\mathbf{q}}e^{-i\mathbf{q}\cdot\mathbf{R}_s}, \tag{1}$$

where s denotes the sth lattice site. c_q is the amplitude of the (planar) oxygen concentration wave with wave vector $\mathbf{q}$. $\mathbf{A}_{\mathbf{q}}$, which is the Fourier transform of the displacement field due to a single defect, is determined by three inhomogeneous linear equations:

$$q\lambda_{ijlm}n_jn_lA_{\mathbf{q}m}=\lambda_{ijlm}n_jL_{lm}, \tag{2}$$

where summation is made over twice-repeated indices; λ_{ijlm} are the tensor components of the elastic moduli, n_i are the components of the unit vector $\mathbf{n}=\mathbf{q}/q$, and $L_{lm}=\delta u_{lm}/\delta c_O$ with u_{lm} the components of the strain tensor and c_O the concentration of oxygen atoms in the chain plane, which is 0.5 at $\delta=0$ in $YBa_2Cu_3O_{7-\delta}$. For tetragonal crystals, the tensor components L_{lm} are given by

$$L_{lm}=\frac{1}{d_l}\frac{\partial d_l}{\partial c_O}\delta_{lm}, \tag{3}$$

where d_l is a lattice parameter.

In the present case of $YBa_2(Cu_{1-x}Al_x)_3O_7$ the oxygen atoms in the Cu(1)-O planes may be considered as interstitials in a square Cu lattice where the two equivalent interstices, γ, are at the midpoints of the edges (x and y) of the unit cell. The intensity of the diffuse scattering, when the atomic displacements are small, may then be shown to take approximately the form [22]

$$I(\mathbf{Q})=\sum_{\gamma}N^2\langle|c_{\mathbf{q}}|^2\rangle[F(\mathbf{Q})\times\mathbf{Q}\cdot\mathbf{A}_{\mathbf{q}}^{\gamma}-f_O^{\gamma}(\mathbf{Q})]^2,\quad\gamma=x,y, \tag{4}$$

where $F(\mathbf{Q})$ is the full unit-cell structure factor noted earlier, $f_O^{\gamma}(\mathbf{Q})$ is the structure factor for the oxygen-vacancy lattice, and N is the number of unit cells. For Miller indices $h+k$ even [large $F(\mathbf{Q})$] and small $\mathbf{q}$ (large $\mathbf{A}_{\mathbf{q}}^{\gamma}$), $F(\mathbf{Q})\times\mathbf{Q}\cdot\mathbf{A}_{\mathbf{q}}^{\gamma}\gg f_O^{\gamma}(\mathbf{Q})$, and we can use the following approximation, assuming for the moment a random distribution of oxygens over the Cu(1)-O plane:

$$\frac{I_H(\mathbf{Q})}{N}=c_O(1-c_O)|F(\mathbf{Q})|^2[(\mathbf{Q}\cdot\mathbf{A}_{\mathbf{q}}^{x})^2+(\mathbf{Q}\cdot\mathbf{A}_{\mathbf{q}}^{y})^2]. \tag{5}$$

For small values of q (associated with the asymptotic displacements at large R), in the vicinity of the Bragg peaks, $I_H(\mathbf{Q})$ is called Huang diffuse scattering (HDS) and it will decrease with q as $1/q^2$ [22].

For our preliminary calculation we chose $c_O=0.5$, $L_{11}=-L_{22}=0.011$, and $L_{33}=0.010$ (these numbers from Ref. [27] were slightly adjusted to give an averaged value of $L_{11}=-L_{22}$ at the O_7 concentration for $x=0$ where the lattice is, of course, orthorhombic; the exact values, however, are not crucial at this point). λ_{ijlm} are usually written as C_{ij}, the elastic constants, which are given by Reichardt *et al.* [23] for the parent compound ($x=0$). Figures 2(d)–2(f) show the results of the calculation of $I_H(\mathbf{Q})/N|F(\mathbf{Q})|^2$ in Eq. (5). The plots cover the same regions of reciprocal space as the data in Figs. 2(a)–2(c) and are plotted in roughly logarithmic intervals. It is clear that, while major features of the data are reproduced, the agreement is particularly unsatisfactory for selected directions about each Bragg point. Nonetheless the essential $\langle 110\rangle$:$\langle 1\bar{1}0\rangle$ shear character of the displacement field is revealed in Figs. 2(d)–2(f).

The thermal diffuse scattering (TDS), however, is not negligible at room temperature. In the one-phonon approximation, TDS per unit cell takes the form [28]

$$\frac{I_T(\mathbf{Q})}{N}=|F(\mathbf{Q})|^2\frac{kT}{v_c}\frac{Q^2}{q^2}\sum_{i=1}^{3}\frac{(\varepsilon_{i,j}g_j)^2}{\rho V_i^2}, \tag{6}$$

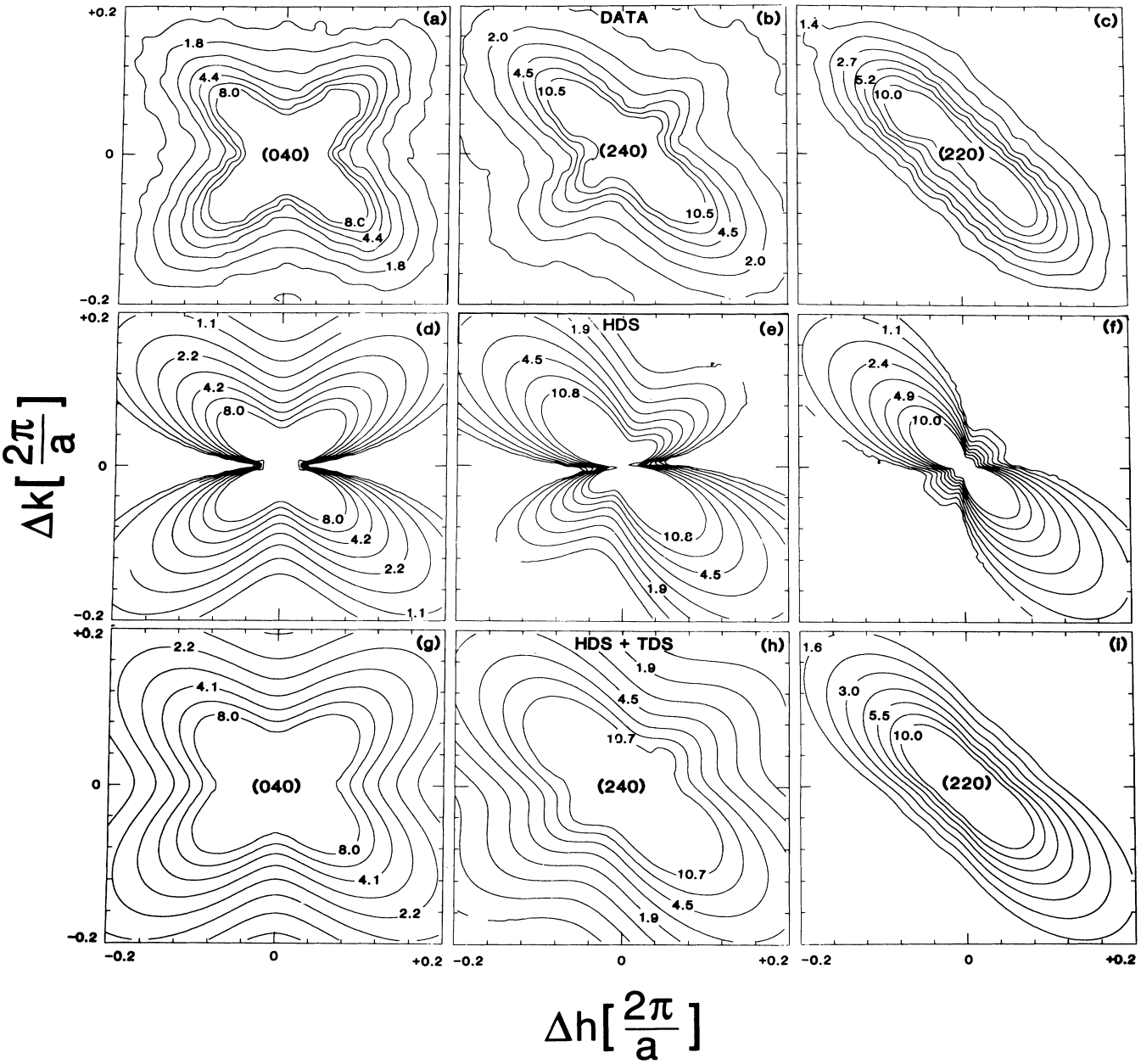

FIG. 2. Contour plots in roughly logarithmic intervals of (a)–(c) the measured x-ray intensity, divided by $|F(\mathbf{Q})|^2$, around (040), (240), and (220) reciprocal-lattice points; (d)–(f) the Huang diffuse scattering (HDS) calculated using Eq. (5); (g)–(i), the combined HDS and TDS [thermal diffuse scattering, Eq. (6)]. The data and calculations are placed on the same basis using a single proportionality constant.

where v_c is the volume of the unit cell, and the g_j are components of the unit vector $\mathbf{g}=\mathbf{Q}/Q$. ρ is the density of the crystal and $\varepsilon_{i,j}$ are the components of the polarization vectors associated with a phonon velocity V_i which may be calculated for a general crystal direction [28]. Again, we must note that the elastic constants, and thus the TDS, demonstrate no particular $\langle 110\rangle$:$\langle 1\bar{1}0\rangle$ shear softness, even at $x=0$, for either the O_6 or O_7 concentration [23].

Taken together, Eqs. (5) and (6) give the total diffuse intensity per unit cell, $I(\mathbf{Q})=[I_H(\mathbf{Q})+I_T(\mathbf{Q})]/N$, which is shown in Figs. 2(g)–2(i) using a single proportionality constant to put data and calculation on the same basis. The agreement with the x-ray diffuse scattering is now quite good, especially in retrieving the radial scattering around (220) and the transverse ($\mathbf{Q}\perp\mathbf{q}$) scattering at

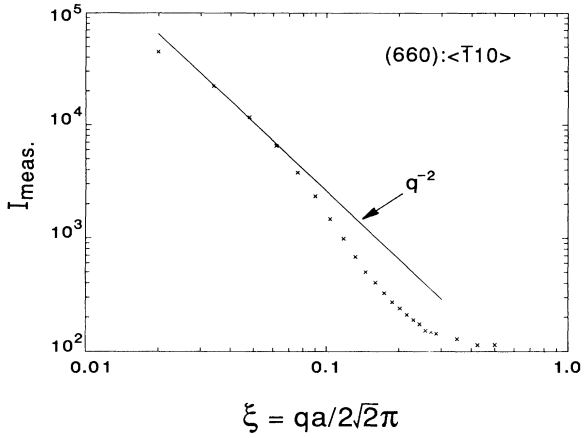

FIG. 3. Measured x-ray intensity vs reduced wave vector $\xi = qa/2\sqrt{2}\pi$ in the $\langle \bar{1}10 \rangle$ direction at the (660) point. The deviation from the expected q^{-2} dependence is attributed to nonrandom short-range oxygen chain ordering (see Ref. [29]) which modifies the HDS but not the TDS. At very small ξ (< 0.03), resolution corrections become important.

(040). However, Fig. 3 shows clearly that the observed diffuse intensity deviates at larger q from the $1/q^2$ behavior [22] associated with both $I_H(\mathbf{Q})$ and $I_T(\mathbf{Q})$. [From the dispersion curves of Reichardt *et al.* [23] we estimate that the $1/q^2$ regime extends to at least $\xi \simeq 0.25$ for the relevant shear modes.] This indicates that $\langle |c_{\mathbf{q}}|^2 \rangle$ is not constant but falls off as q increases [29], and work on the detailed evaluation of $\langle |c_{\mathbf{q}}|^2 \rangle$ is currently in progress. A rough estimate from Fig. 3 of the correlation range for this local chain order is ~ 40 Å which is considerably greater than the planar coherence length of ~ 15 Å for superconductivity in this material [25]. In other words, as far as the paired carriers are concerned, the structure is (locally) orthorhombic. In this connection we note also recent work on the importance of ordered oxygen chains for high T_c in $YBa_2Cu_3O_{7-y}$ [30,31].

This work was supported by the NSF on DMR-8903339 and the State of Texas at the Texas Center for Superconductivity at the University of Houston. This research was performed in part at the Oak Ridge National Laboratory beam line X14 at the National Synchrotron Light Source, Brookhaven National Laboratory, sponsored by the Division of Materials Sciences and Division of Chemical Sciences, U.S. Department of Energy and under Contract No. DE-AC05-840R21400 with the Martin Marietta Energy System, Inc. We wish to thank Y. Zhu for our crystals and for discussions of his TEM results. P.W. also thanks the Deutsche Forschungsgemeinschaft for partial support.

[1] T. J. Kistenmacher, Phys. Rev. B **38**, 8862 (1988).
[2] T. Takabatake and M. Ishikawa, Solid State Commun. **66**, 413 (1988).
[3] Y. Maeno *et al.*, Jpn. J. Appl. Phys. **26**, L1982 (1987).
[4] H. Obara *et al.*, Jpn. J. Appl. Phys. **27**, L603 (1988).
[5] E. Takayama-Muromachi *et al.*, Jpn. J. Appl. Phys. **26**, L2087 (1987).
[6] T. Siegrist *et al.*, Phys. Rev. B **36**, 8365 (1987).
[7] J. M. Tarascon *et al.*, Phys. Rev. B **37**, 7458 (1988).
[8] P. Bordet *et al.*, Solid, State Commun. **66**, 435 (1988).
[9] C. Y. Yang *et al.*, Phys. Rev. B **39**, 6681 (1989).
[10] A. Koizumi *et al.*, Jpn. J. Appl. Phys. **28**, L203 (1989).
[11] F. Bridges *et al.*, Phys. Rev. B **39**, 11 603 (1989).
[12] C. Saragovi-Badler *et al.*, Solid State Commun. **66**, 381 (1988).
[13] S. Suharan *et al.*, Solid State Commun. **70**, 817 (1989).
[14] Y. Zhu *et al.*, Ultramicroscopy (to be published).
[15] Y. Zhu *et al.*, Philos. Mag. Lett. **62**, 51 (1990).
[16] X. Jiang, Ph.D. thesis, University of Houston (unpublished).
[17] T. Krekels *et al.*, Physica C (to be published).
[18] Z. Cai and S. D. Mahanti, Phys. Rev. B **40**, 6558 (1989).
[19] G. Baumgärtel and K. H. Bennemann, Phys. Rev. B **40**, 6711 (1989).
[20] E. Salomons and D. de Fontaine (to be published).
[21] C. P. Burmester *et al.*, Solid State Commun. **77**, 693 (1991).
[22] M. A. Krivoglaz, *Theory of X-Ray and Thermal Neutron Scattering by Real Crystals* (Plenum, New York, 1969).
[23] W. Reichardt *et al.*, Supercond. Sci. Technol. **1**, 173 (1988); Physica (Amsterdam) **162-164C**, 464 (1989).
[24] See *Proceedings of the Workshop on First-Order Displacive Phase Transformations,* edited by L. E. Tanner and M. Wuttig [Mat. Sci. Eng. A **127** (1990)]; S. M. Shapiro *et al.*, Phys. Rev. Lett. **57**, 3199 (1986); I. M. Robertson and C. M. Wayman, Philos. Mag. A **48**, 421 (1983); **48**, 443 (1983); **48**, 629 (1983).
[25] Y. Xu and M. Suenaga, Phys. Rev. B **43**, 5516 (1991).
[26] Y. Zhu *et al.* (to be published).
[27] S. Nakanishi *et al.*, Jpn. J. Appl. Phys. **27**, L329 (1988).
[28] W. A. Wooster, *Diffuse X-Ray Reflections from Crystals* (Oxford Univ. Press, New York, 1962).
[29] The scattering off the oxygen-vacancy concentration fluctuations in this structure is centered on Bragg reflections and may be calculated within the formalism outlined by D. de Fontaine *et al.*, Phys. Rev. B **36**, 5709 (1987). It may be measured, as in Fig. 3, even when $f_O(\mathbf{Q})$ in Eq. (4) is negligible, through its presence in the correlated displacement scattering.
[30] J. D. Jorgensen *et al.*, Physica (Amsterdam) **167C**, 571 (1990).
[31] B. W. Veal *et al.*, Phys. Rev. B **42**, 6305 (1990).